2023

Adaptive Fuzzy Supplementary Controller for SSR Damping in a Series-Compensated DFIG-Based Wind Farm

Mohamed Abdeen
Al-Azhar University, Cairo, Egypt

Sayed Hosny Ahmed El-Banna
Al-Azhar University, Cairo, Egypt

Sara Elgohary
Al-Azhar University, Cairo, Egypt

See next page for additional authors

Funder: European Union's Horizon 2020 Research and Enterprise Ireland through the Marie Sklodowska-Curie (Grant Number: 847402)

IEEE Access
Multidisciplinary ⋮ Rapid Review ⋮ Open Access Journal

Received 18 November 2022, accepted 24 December 2022, date of publication 28 December 2022,
date of current version 5 January 2023.

Digital Object Identifier 10.1109/ACCESS.2022.3232983

RESEARCH ARTICLE

Adaptive Fuzzy Supplementary Controller for SSR Damping in a Series-Compensated DFIG-Based Wind Farm

MOHAMED ABDEEN[1], SAYED HOSNY AHMED EL-BANNA[1], SARA ELGOHARY[1], HEND MOSTAFA[1], NORA GHALY[1], NOURHAN ADEL[1], ZEINAB ELKHWAS[1], MOHAMED ALAHMADY[1], HOSSAM M. ZAWBAA[2,3,4], AND SALAH KAMEL[5]

[1]Department of Electrical Engineering, Faculty of Engineering, Al-Azhar University, Cairo 4434003, Egypt
[2]Faculty of Computers and Artificial Intelligence, Beni-Suef University, Beni Suef 2722165, Egypt
[3]CeADAR Ireland's Center for Applied AI, Technological University Dublin, Dublin 8, D07 EWV4 Ireland
[4]Applied Science Research Center, Applied Science Private University, Amman 11931, Jordan
[5]Electrical Engineering Department, Faculty of Engineering, Aswan University, Aswan 81542, Egypt

Corresponding authors: Mohamed Abdeen (abdeenm88@yahoo.com) and Hossam M. Zawbaa (hossam.zawbaa@gmail.com)

The work of Hossam M. Zawbaa was supported by the European Union's Horizon 2020 Research and Enterprise Ireland through the Marie Skłodowska-Curie under Grant 847402.

ABSTRACT Although using a series compensation technique in a long transmission line effectively increases the transmittable power; it may cause a sub-synchronous resonance (SSR) phenomenon. Gate-controlled series capacitor (GCSC) is an effective method for SSR damping by controlling the turn-off angle. In the previous studies, a constant supplementary damping controller (SDC) was used for controlling the turn-off angle, which can mitigate the SSR phenomenon. However, these methods can not capture the maximum transmittable power at different operating points. In this paper, a fuzzy logic controller (FLC) is proposed to compute the gain of SDC based on the wind speed and the error between the measured and reference line currents for transferring as much power as possible and damping the SSR phenomenon simultaneously. Using the MATLAB/SIMULINK program, the proposed method is tested at different operating points to validate its effectiveness and robustness. Compared to the traditional method (constant SDC), the maximum transmittable power, as well as SSR damping, is achieved in all studied cases by the proposed method (variable SDC).

INDEX TERMS Sub-synchronous resonance (SSR), gate-controlled series capacitor (GCSC), adaptive fuzzy supplementary controller, stability.

I. INTRODUCTION

Series compensation is the most effective and economical method for increasing the transmittable power in long transmission lines by partially canceling the transmission line reactance. However, it was proven that the high compensation levels and low wind speeds have a detrimental effect on safety and system stability. This phenomenon is known as a sub-synchronous resonance (SSR) [1], [2]. The SSR phenomenon is a general term where the series-compensated transmission line exchanges energy with a generator at one or more frequencies less than the synchronous frequency (50 or 60 Hz) [1], [3]. A doubly-fed induction generator (DFIG) is the most commonly used because it can extract the maximum power at variable wind speeds. On the basis of the previous studies, the high compensation levels, low wind speeds, and system parameters (larger gains of the rotor-side converter (RSC) of DFIG) have a detrimental impact on the system stability [1], [4], [5], [6], [7]. With increasing the gains of the RSC,the equivalent rotor resistance is a negative value and larger than the stator and network resistances. Thus, thetotal resistance is negative, leading to the appearance of the SSR [4], [5], [6], [7].

Many stations around the world have experienced SSR events [8], [9], [10]. For example, in 1970 and 1971, the Mohave power station experienced the SSR phenomenon,

The associate editor coordinating the review of this manuscript and approving it for publication was Shun-Feng Su.

which damaged their shaft system [10]. On March 19, 2013, the SSR phenomenon was detected at the Guyuan substation. To avoid the dangerous risks of the SSR, many wind turbines have been shut down@comm and one of the series capacitors has been canceled [9]. It should be mentioned that around 58 SSR events were detected only from December 2012 to December 2013 [9].

For taking the full benefits of the series compensation and keeping the system stable at the same time, the researchers have proposed using a flexible AC transmission system (FACTS) series compensation or adding a supplementary damping controller (SDC) to the DFIG-converter controllers [2], [11], [12], [13]. It should be noted that the series FACTS has already been installed in many stations around the world for power-flow control and power oscillation damping [14], [15].

Among the series FACTS devices, the gate-controlled series capacitor (GCSC) is the most interesting in SSR damping because of its simplicity and flexibility [14], [16]. Improving the control of the GCSC is very important to enhance the system stability under different operating conditions [17]. In [18], a GCSC was used for mitigating the SSR. The measured active power is applied to a low pass filter to calculate the power deviation ΔP, which is fed to a proportional gain block. The output of the proportional gain@comm $\Delta\gamma$a, is subtracted from the steady-state turn-off angle γ_0 to generate the turn-off angle γ for SSR damping. Also, the impact of the rating of the GCSC on the system stability was studied. In [19], a constant power control (CPC) methodology with GCSC was presented for SSR damping. The difference between the instantaneous measured active power and the reference active power is applied to the PI controller. Then, the output of the PI controller is added to the steady-state turn-off angle 113.5^0 However, the system lacks stability at low wind speeds and high compensation levels.

In [20] and [21], a supplementary damping controller (SDC) was added to the traditional method [19] to improve the system's stability. Both the line current, rotor speed, and capacitor voltage were tested as an input control signal (ICS) to the SDC using residue-based analysis and root locus diagram. The results showed that: 1) a very large gain, $K_{SDC} = 27000$, is needed to damp the SSR when the rotor speed is used as an ICS [22]. 2) a smaller gain is required for the line current and capacitor voltage to mitigate the SSR. Given that the series compensation could be far from the location of the GCSC, the communication links are needed to transfer the capacitor voltage signal, or it should be estimated. Whereas the line current is calculated based on the measured three-phase voltages and three-phase currents [20]. The current signal was used as an effective signal for damping the SSR in [4], [20], and [21]. In this study, the line current was used as an input signal to the SDC. Since the gain of SDC is a constant value, it is designed at the worst case (high compensation level & low wind speed) to ensure that the system remains stable. However, this method can not capture the maximum transmittable power at different operating points.

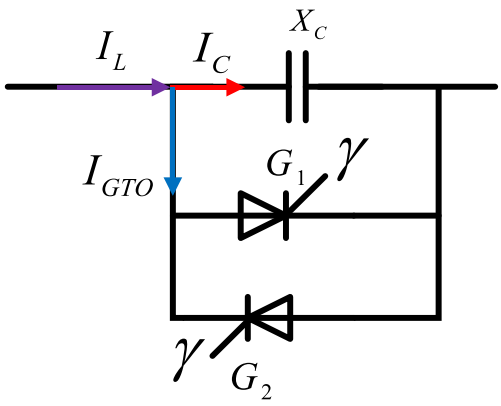

FIGURE 1. GCSC circuit diagram.

To address the previous issues, this paper presents a fuzzy logic controller to compute the SDC gain according to the operating point for capturing the maximum transmittable power and SSR damping in a series-compensated DFIG-based wind farm. The main contributions of this work can be summarized in the following points:

1) The appropriate SDC gain according to each operating point is computed by FLC for capturing the maximum transmittable power and SSR damping, unlike the previous studies, where the SDC gain is a constant value.
2) The impact of SDC gain on the transferred power, in terms of the turn-off angle of GCSC, and the SSR damping is investigated at different operating points, unlike the previous studies, where the authors only focused on SSR mitigation.
3) The proposed method is compared to the traditional method in terms of the turn-off angle and SSR damping at different wind speeds.

The rest of the paper is organized as follows. Gate-controlled series capacitor is explained in Section II. The SSR damping method is described in Section III. The power system model is given in Section IV. Simulation results and discussions are presented in Section V. Performance comparison with a recent SSR damping method is introduced in Section VI. Finally, the conclusion of this work is drawn in Section VII.

II. GATE-CONTROLLED SERIES CAPACITOR (GCSC)

Fig. 1. shows the block diagram of GCSC, which consists of a fixed capacitor (X_c) in parallel with a pair of GTO thyristors [23].

where I_c, I_L, and I_{GTO} represent the capacitor current, line current, and GTO thyristor current, respectively. γ represents the turn-off angle and it is measured from the zero crossings of the line current. The effective reactance of the GCSC (X_{GCSC}) in terms of the turn-off angle is shown in Fig. 2, and

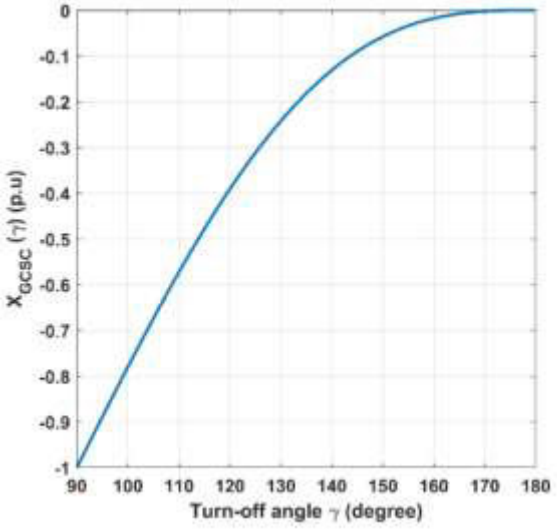

FIGURE 2. Effective reactance of the GCSC as a function of turn-off angle γ (degree).

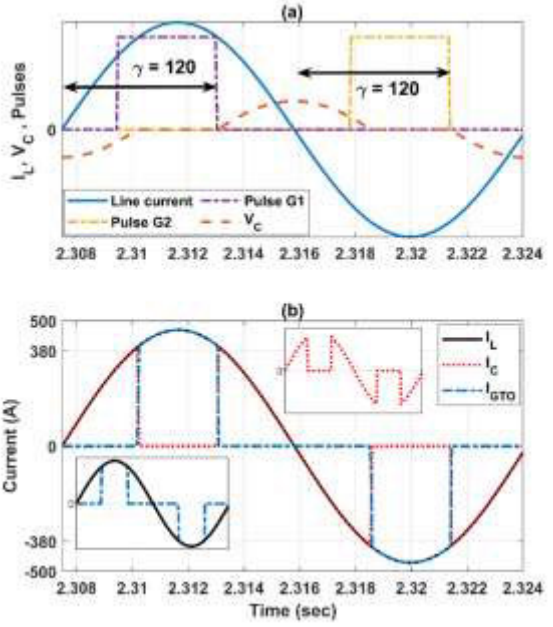

FIGURE 3. GCSC waveforms for $\gamma = 120^0$ (a) Line current, capacitor voltage, and pulses (b) Line current, capacitor current, and GTO current.

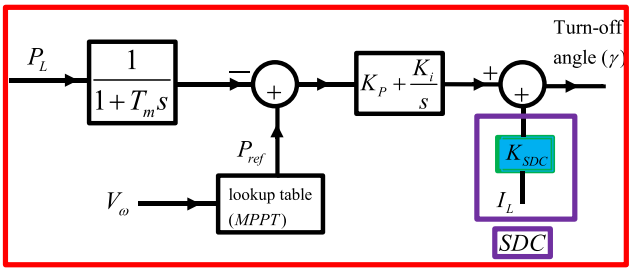

FIGURE 4. Traditional method for SSR damping [20].

can be calculated as [15] and [23]:

$$X_{GCSC}(\gamma) = \frac{X_C}{\pi}(2\gamma - 2\pi - \sin(2\gamma)) \tag{1}$$

It can be noted that as the γ changes from 90° to 180°, X_{GCSC} varies from X_C to zero. Based on the above equation, the effective reactance of the GCSC is equal to the fixed capacitor ($X_{GCSC} = X_C$) when $\gamma = 90^0$. Thus, no current passes in the GTO, the GTO valve is opened, whereas the line current passes through the capacitor of GCSC ($I_L = I_c$). On the other hand, the effective reactance of the GCSC equals zero when $\gamma = 180^0$. Thus, no current passes through the GCSC's capacitor (I_c = zero), the capacitor is completely canceled, whereas the line current passes through the GTO ($I_{GTO} = I_L$) where the GTO valve is fully closed [23].

Fig. 3 shows the GCSC waveforms when the turn-off angle equals 120^0. The line current, pulses, and capacitor voltage are shown in Fig. 3a, whereas the line current, GTO current, and capacitor current are shown in Fig. 3b. It can be observed that: 1) the GTO valve is closed automatically when the capacitor voltage reaches zero and it is still closed until the pulse is removed. 2) the capacitor current equals zero (value) when the GTO valve is closed (opened). 3) the line current equals the sum of the capacitor current and GTO current.

III. SSR DAMPING METHOD

A. TRADITIONAL METHOD

Fig. 4 shows the block diagram of the traditional method [20], [21]. The measured active power passes through the low-pass filter. Then, it is compared to the reference active power, and the error passes through the PI controller.

As stated earlier in [19] and [24], this constant power control (CPC) methodology may not be adequate for damping the SSR at low wind speeds and high compensation levels. Thus, an auxiliary SDC is added to the CPC methodology to damp the SSR, as shown in Fig. 4. The line current is used as an input signal to the SDC, and can be calculated as follows:

$$I_L = \frac{\sqrt{P_L^2 + Q_L^2}}{V_S} \tag{2}$$

where P_L, Q_L, and V_S represent the transmission line active power, the transmission line reactive power, and line voltage. Both the measured three-phase voltages and three-phase currents are needed to obtain P_L, Q_L, and V_S. It should be noted that the K_{SDC} is a constant value and it is selected at the worst operating condition (lowest wind speed and highest compensation level). The relation between the K_{SDC}, the turn-off angle and system stability at different wind speeds will be explained later.

B. PROPOSED METHOD

The main goal of this method is to calculate the SDC gain according to the operating point using the fuzzy logic controller for increasing the transmittable power with keeping the system stable [25], as shown in Fig. 5.

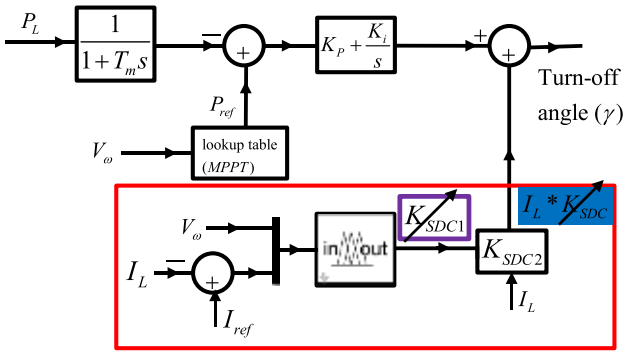

FIGURE 5. Adaptive Fuzzy SDC for SSR damping.

TABLE 1. Fuzzy rules for computing K_{SDC1}.

Error	Wind speed		
	Low	Medium	High
NB	H	M	S
NM	M	S	VS
NS	S	VS	VS
Z	VS	VS	VS
PS	S	VS	VS
PM	M	S	VS
PB	H	M	S

As shown in Fig. 5, the K_{SDC1} is calculated based on the wind speed and the error between the measured and reference currents by FLC. Then, K_{SDC1} is multiplied by K_{SDC2} (11.5) to obtain K_{SDC}, and can be written as:

$$K_{SDC} = K_{SDC1} * K_{SDC2} \tag{3}$$

FLC has two inputs, namely, wind speed and the error between the measured and reference line currents, whereas the output of FLC is K_{SDC1}.

C. FUZZY CONTROL METHODOLOGY

The fuzzy logic controller (FLC) is a mathematical tool for dealing with imprecise inputs and can handle nonlinearity. Moreover, the FLC covers a wider range of operating conditions, unlike the conventional controller. Thus, it has been applied in many applications [26], [27], [28]. The design process of the FLC is described as follows.

1) FUZZIFICATION

Fuzzification is the process of converting the crisp data, wind speed and error, into fuzzy data using membership functions, as shown in Fig. 6a and Fig. 6b. The error is represented by seven membership functions, as shown in Fig. 6a, whereas the wind speed is represented by three membership functions as shown in Fig. 6b. Based on the wind speed and error, the grade of membership values are determined. On the other hand, the membership functions of the output signal (K_{SDC1}) is shown in Fig. 6c. Membership functions were obtained by the trial-and-error method. The range of error, wind speed, and K_{SDC1} are [−0.150.15], [710], and [06], respectively.

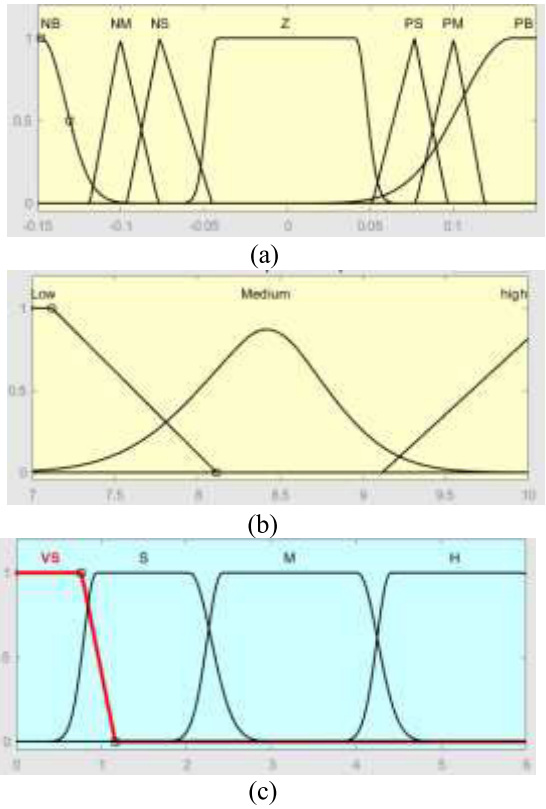

FIGURE 6. Membership functions for (a) error, (b) wind speed, and (c) K_{SDC1}.

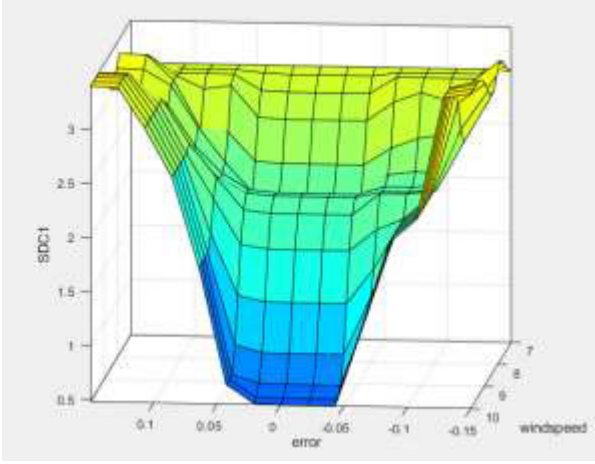

FIGURE 7. Fuzzy control three-dimensional map.

2) FUZZY CONTROL RULES

It is the heart of an FLC. These rules are designed based on good knowledge of the problem. The fuzzy rule is represented by a sequence of the form IF-THEN, leading to algorithms describing what action or output should be taken (K_{SDC1}) in terms of the currently observed information (wind speed & error). It should be noted that the "Or" operation method is used in this study. For example, IF the wind speed is low, or the error is NB, THEN the output (K_{SDC1}) is high. Given

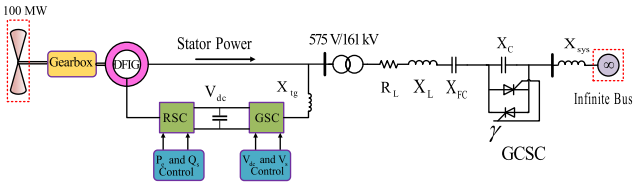

FIGURE 8. Modified IEEE first benchmark model for a DFIG-based wind farm with the GCSC.

that the error is represented by seven membership functions and the wind speed is represented by three membership functions, the total fuzzy control rules of computing $K_{SDC}1$ equal 21 as shown in Table 1.

3) DEFUZZIFICATION

In this part, the fuzzy output is converted to the crisp output because the real applications only deal with the crisp value. The final output (crisp value) is the weighted average of all rule outputs and can be written as:

$$\text{Final output}=\frac{\sum_{n=1}^{21}\mu_n z_n}{\sum_{n=1}^{21}\mu_n} \tag{4}$$

where μ_n is the fuzzy output of each rule, z_n is the crisp output of each rule. It should be noted that the center of gravity method (COG) is used to determine the crisp value according to each fuzzy output of each rule. The three-dimensional diagram between the inputs and output is shown in Fig. 7.

IV. POWER SYSTEM MODEL

For an assessment of the performance of the proposed method, the IEEE first benchmark model (FBM) is adapted with a doubly-fed induction generator in the MATLAB/SIMULINK program, as shown in Fig. 8. This model has been widely employed in several research papers for SSR studies [2], [13], [20], [21], [29], [30]. This system includes a 100 MW DFIG-based wind farm, a step-up transformer, a series-compensated transmission line, GCSC, and an infinite bus. The wind farm includes 67 wind turbine units, where the power rating of each unit is 1.5 MW. The model parameters are listed in Appendix.

V. SIMULATION RESULTS AND DISCUSSIONS

In order to validate the proposed method's capability for damping the SSR phenomenon and capturing the max transmittable power, it is tested at different wind speeds ($V_\omega = 7$ m/s, $V_\omega = 8$ m/s, $V_\omega = 9$ m/s, and $V_\omega = 10$ m/s). Moreover, the performance of the traditional method without SDC, the traditional method [20], [21], and the proposed method are presented to prove its effectiveness and robustness. In this study, the fixed series capacitor (X_{FC}), and the GCSC (X_C) represent 70 %, and 30 % of the total compensation level, respectively. Initially, the system is stable where the compensation level is low (K= 10 %). Then, at

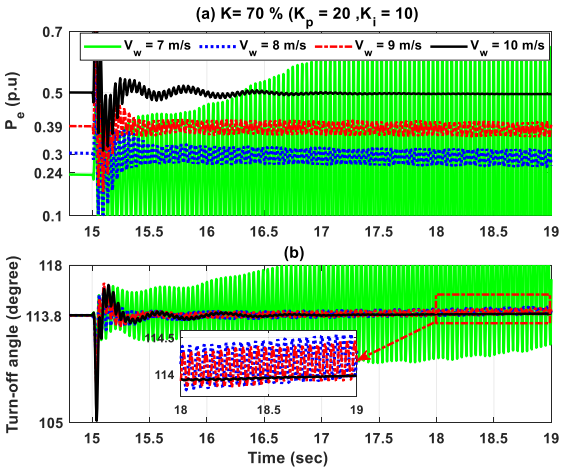

FIGURE 9. Performance of the traditional method without SDC.

$t = 15$ sec, the compensation level is increased to 70 % in all studied cases.

A. TRADITIONAL METHOD WITHOUT SDC

The performance of the traditional method without SDC for $V_\omega = 7$ m/s, $V_\omega = 8$ m/s, $V_\omega = 9$ m/s, and $V_\omega = 10$ m/s is shown in Fig. 9. The generated active power of DFIG, and the turn-off angle of GCSC are plotted.

The following notes can be extracted from Fig. 9:

1) The system lacks stability for $V_w = 7$ m/s, $V_w = 8$ m/s, and V_w =9 m/s. That is to say, the lower the wind speed, the higher the oscillation's amplitude and the more the system instability.
2) The system is stable for V_w= 10 m/s, where the traditional method without SDC consumed around three seconds for SSR damping.
3) The traditional method without SDC can not damp the SSR at high compensation levels and low wind speeds.

B. TRADITIONAL METHOD (CONSTANT SDC)

The simulation is repeated again for $V_\omega = 7$ m/s, $V_\omega = 8$ m/s, and $V_\omega = 9$ m/s when the traditional method [20], [21] is in use, as illustrated in Figs. 10, 11, and 12, respectively.

The following conclusions can be drawn from Figs. 10–12:

1) For $V_w = 7$ m/s, $V_w = 8$ m/s, and $V_w = 9$ m/s, the system is stable when $K_{SDC} = 34$, $K_{SDC} = 24$, and $K_{SDC} = 18$, respectively. That is to say; a larger SDC gain is required when the wind speed decreases for damping the SSR phenomenon.
2) Fig. 10 shows that the smaller the SDC gain ($K_{SDC} = 28$, $K_{SDC} = 22$, and $K_{SDC} = 14$), the smaller the turn-off angle (120.5^0, 119^0, 117^0) and the lower the system stability. On the other hand, the system is stable when $K_{SDC} = 34$, where the turn-off angle equals 122^0.
3) The larger the SDC gain, the higher the turn-off angle. Consequently, the effective reactance of GCSC decreases (Eq.1), and thus the total compensation level

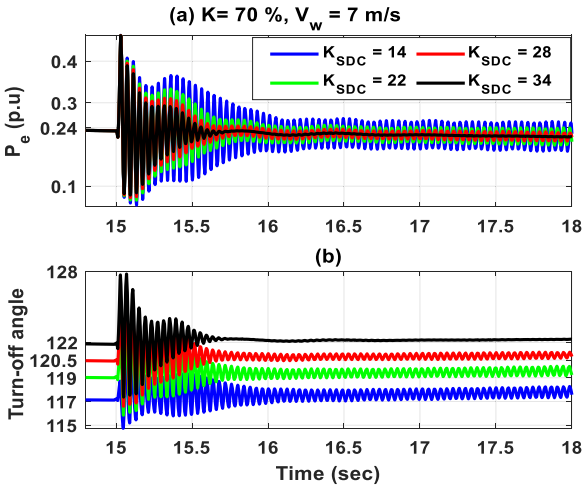

FIGURE 10. Impact of increasing the SDC gain at 7 m/s wind speed and 70 % compensation level.

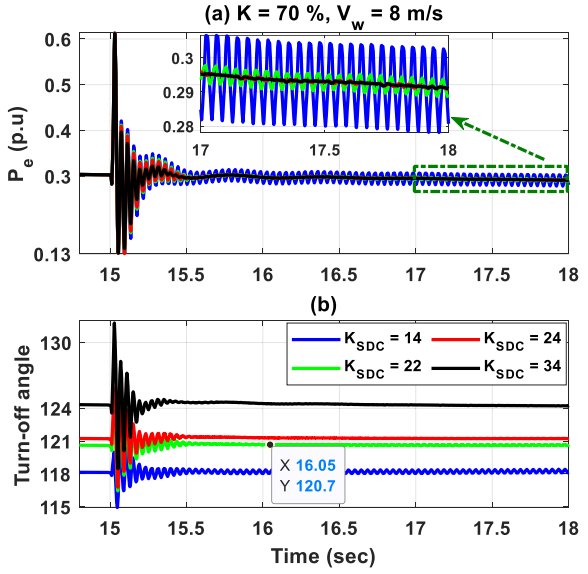

FIGURE 11. Impact of increasing the SDC gain at 8 m/s wind speed and 70 % compensation level.

(X_{TC}) decreases, which leads to a decrease in the transmittable power according to $P = \frac{V_S * V_R}{X_L - X_{TC}} sin\delta$

4) At constant SDC gain, e.g. $K_{SDC} = 22$, the higher the wind speed, the higher the turn-off angle, as shown in Figs. 10, 11, and 12. Thus, less power is transferred.
5) These results prove the importance of using variable SDC gain instead of a constant SDC gain for capturing max transmittable power according to the operating point.

C. PROPOSED METHOD (VARIABLE SDC)

In this subsection, the performance of the proposed method (variable SDC gain) is compared to the traditional method (constant SDC gain) for $V_\omega = 7$ m/s, $V_\omega = 8$ m/s, $V_\omega = 9$ m/s, and $V_\omega = 10$ m/s, as shown in Figs. 13, 14, 15, and 16,

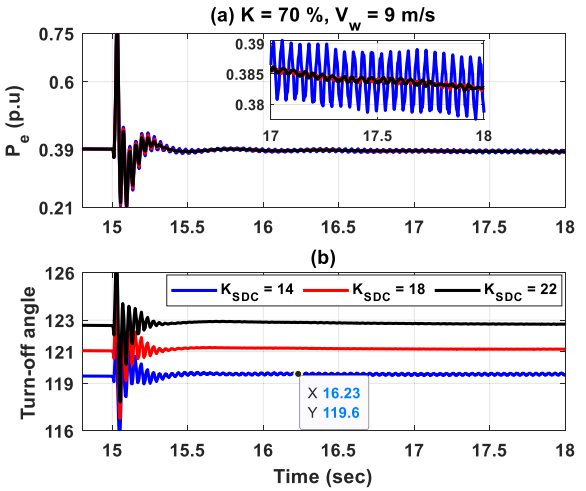

FIGURE 12. Impact of increasing the SDC gain at 9 m/s wind speed and 70 % compensation level.

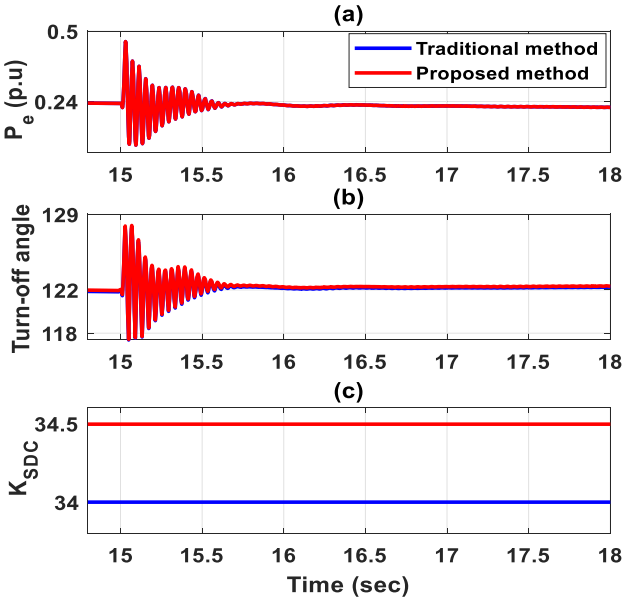

FIGURE 13. Electric power, turn-off angle, and K_{SDC} when K= 70 % and $V_w = 7$ m/s.

respectively. The generated active power of DFIG, the turn-off angle of the GCSC, and the K_{SDC} are depicted.

The following observations can be drawn from Figs. 13–16:

1) When the traditional method (constant SDC gain) is activated [20], [21], the turn-off angle is equal to 122^0, 124^0, 128^0, and 132^0 for $V_w = 7$ m/s, $V_w = 8$ m/s, $V_w = 9$ m/s, and $V_w = 10$ m/s, respectively. Given that the system becomes more stable with increasing the wind speed [1], it is supposed that the turn-off angle decreases, and thus the percentage of the total compensation level increases. However, these results show that the turn-off angle increases when the

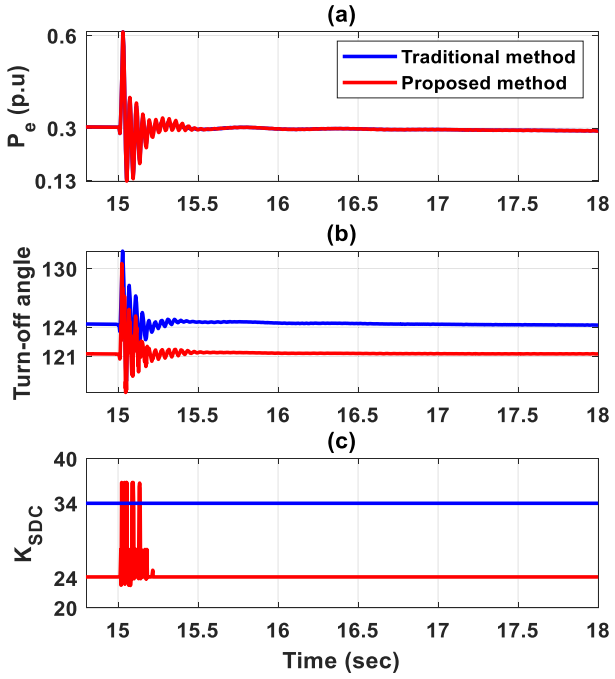

FIGURE 14. Electric power, turn-off angle, and K_{SDC} when K= 70 % and $V_w = 8$ m/s.

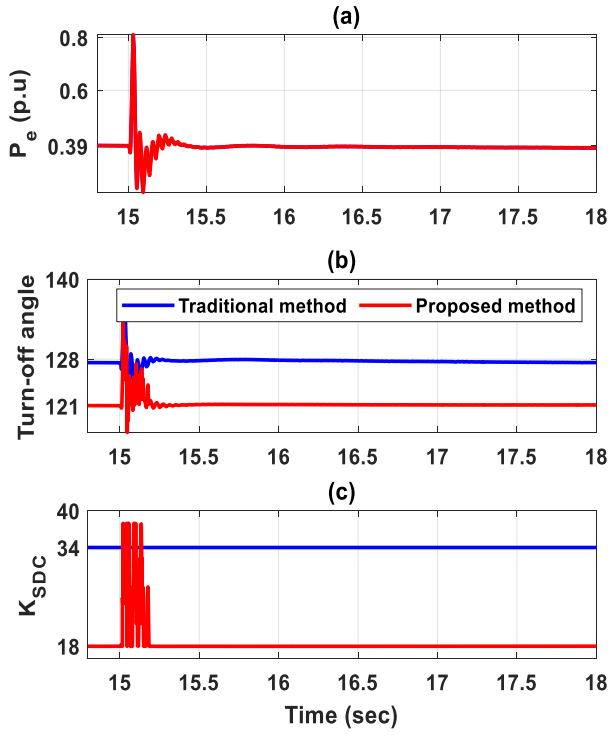

FIGURE 15. Electric power, turn-off angle, and K_{SDC} when K= 70 % and $V_w = 9$ m/s.

wind speed increases, and thus the transmittable power decreases.

2) When the proposed method (variable SDC gain) is in use, the turn-off angle is equal to 122^0, 121.5^0, 120.8^0, and 117^0 for $V_w = 7$ m/s, $V_w = 8$ m/s, $V_w = 9$ m/s, and $V_w = 10$ m/s, respectively. That is to say, the higher the wind speed, the smaller the K_{SDC} and the lower the turn-off angle. Thus, the percentage of the total compensation level increases and more power is transferred.
3) With the traditional method, the SDC gain equals 34 in all studied cases. On the other hand, the computed SDC gain by the proposed method is equal to 34.5, 24, 18, and 5 for $V_w = 7$ m/s, $V_w = 8$ m/s, $V_w = 9$ m/s, and $V_w = 10$ m/s, respectively.
4) The proposed method (variable SDC gain) has the same performance as the traditional method for SSR damping with a lower turn-off angle in all studied cases, leading to a higher effective reactance of the GCSC. Thus, more power is transferred via the long transmission line.

TABLE 2. Comparison between the proposed method and the traditional method (X_{FC}= 0.245*p.u*) (X_{TC}=X_{FC}+X_{GCSC}).

Wind speed V_ω	Traditional method [20, 21] (Constant SDC)				Proposed method (Variable SDC)			
	K_{SDC}	Turn-off angle γ	$X_{GCSC}(\gamma)$ p.u	X_{TC} p.u	K_{SDC}	Turn-off angle γ	$X_{GCSC}(\gamma)$ p.u	X_{TC} p.u
7 m/s	34	122^0	0.037	0.282	34.5	122^0	0.037	0.282
8 m/s	34	124^0	0.034	0.279	24	121.5^0	0.038	0.283
9 m/s	34	128^0	0.028	0.273	18	120.8^0	0.04	0.285
10 m/s	34	132^0	0.023	0.268	5	117^0	0.046	0.29

Table 2 introduces a summary comparison between the proposed method and the traditional method [20], [21] in terms of the SDC gain, the turn-off angle, the effective reactance of the GCSC, and the total compensation level. In this study, $X_C = 27.3\Omega$. The base value of $X_{base} = V_{base}^2 / S_{base} = (161000)^2 / (100 * 10^6) = 259\Omega$. Based on Eq. (1), the effective reactance of GCSC can be calculated according to the turn-off angle, as shown in Table 2. The total compensation level, X_{TC}, equals X_{FC} plus X_{GCSC}. It should be noted that X_{FC} is a constant value, whereas X_{GCSC} depends on the turn-off angle. Thereby, the total compensation level is not a constant value. Table 2 shows that the total compensation level is proportional to the wind speed when the proposed method is activated, whereas the total compensation level is inversely proportional to the wind speed when the traditional method is in use. Thus, more power is transferred by the proposed method compared to the traditional method.

VI. PERFORMANCE COMPARISON

The capability of the proposed method is compared to a recent method [2] for damping the SSR phenomenon. In [2], an SDC is integrated into the RSC's inner control loops of DFIG. The SDC comprises a first-order low-pass filter block, two-stage phase compensation blocks, and a gain block. The rotor voltage was used as an input signal [2]. As shown in Fig. 17, the proposed method has the best performance for alleviating the SSR, where less time for damping the SSR is achieved by the proposed method.

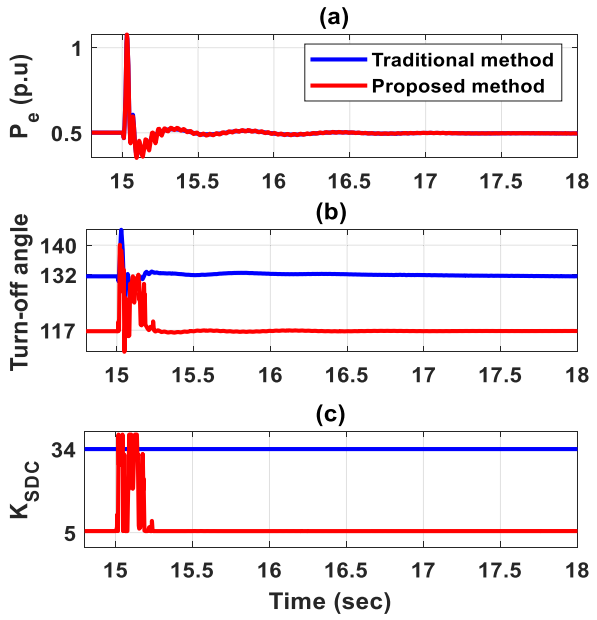

FIGURE 16. Electric power, turn-off angle, and K_{SDC} when K= 70 % and V_w = 10 m/s.

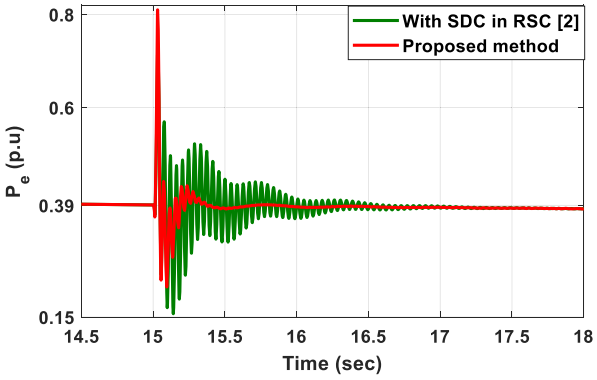

FIGURE 17. Electric power at 9 m/s wind speed and 70 % compensation level.

VII. CONCLUSION

In this paper, an adaptive fuzzy supplementary controller for damping the SSR phenomenon and capturing the max transmittable power in a series-compensated DFIG-based wind farm was presented. Based on the wind speed and the error between the measured and reference line currents, the SDC gain was identified using an FLC. The proposed method was tested at $V_\omega = 7$ m/s, $V_\omega = 8$ m/s, $V_\omega = 9$ m/s, and $V_\omega = 10$ m/s. The compensation level is set to 70 % at different wind speeds. Compared to the traditional method (constant SDC gain), the results showed that: 1) a larger SDC gain is required to completely dampen the SSR at different wind speeds when the traditional method is in use. 2) The larger the SDC gain, the higher the turn-off angle. Consequently, the effective reactance of GCSC decreases, and thus the total compensation level decreases, which in turn leads to decreasing the transmittable power. 3) with the traditional method, the turn-off angle is proportional to the wind speed. Thus, the total compensation level decreases. 4) the proposed method (variable SDC gain) has the same performance as the traditional method for SSR damping with a lower turn-off angle in all studied cases, leading to a higher effective reactance of the GCSC. Thus, more power is transferred via the long transmission line. 5) the proposed method has the best performance, where it can successfully dampen the SSR and increase the transferred power at the same time. Experimental validation is left as a future work.

APPENDIX

TABLE 3. Parameters of a single DFIG and the aggregated DFIG.

Rated power	1.5 MW	100 MW
Rated voltage	575 V	575 V
Rated frequency	60 Hz	60 Hz
R_s	0.023	0.023
X_{ls}	0.18	0.18
R_r	0.016	0.016
X_{lr}	0.16	0.16
X_M	2.9	2.9
DC-link voltage	1150 V	1150 V
DC-link capacitor	10000 μF	67*10000 μF

TABLE 4. Parameters of the transmission line.

Transformer ratio	575 V/161 kV
Base power	100 MVA
X_T	0.1
R_L	0.02
X_L	0.5
X_C at 50 % compensation level	64.8 Ω

REFERENCES

[1] M. Abdeen, H. Li, S. Kamel, A. Khaled, M. El-Dabah, M. Kharrich, and H. F. Sindi, "A recent analytical approach for analysis of sub-synchronous resonance in doubly-fed induction generator-based wind farm," *IEEE Access*, vol. 9, pp. 68888–68897, 2021.
[2] M. Abdeen, H. Li, M. A. Mohamed, S. Kamel, B. Khan, and Z. Chai, "Sub-synchronous interaction damping controller for a series-compensated DFIG-based wind farm," *IET Renew. Power Gener.*, vol. 16, no. 5, pp. 933–944, Apr. 2022.
[3] J. Shair, X. Xie, J. Yang, J. Li, and H. Li, "Adaptive damping control of subsynchronous oscillation in DFIG-based wind farms connected to series-compensated network," *IEEE Trans. Power Del.*, vol. 37, no. 2, pp. 1036–1049, Apr. 2022.
[4] P.-H. Huang, M. El Moursi, W. Xiao, and J. Kirtley, "Subsynchronous resonance mitigation for series-compensated DFIG-based wind farm by using two-degree-of-freedom control strategy," *IEEE Trans. Power Syst.*, vol. 30, no. 3, pp. 1442–1454, May 2015.
[5] U. Karaagac, J. Mahseredjian, S. Jensen, R. Gagnon, M. Fecteau, and I. Kocar, "Safe operation of DFIG-based wind parks in series-compensated systems," *IEEE Trans. Power Del.*, vol. 33, no. 2, pp. 709–718, Apr. 2018.

[6] M. Ghafouri, U. Karaagac, H. Karimi, S. Jensen, J. Mahseredjian, and S. O. Faried, "An LQR controller for damping of subsynchronous interaction in DFIG-based wind farms," *IEEE Trans. Power Syst.*, vol. 32, no. 6, pp. 4934–4942, Nov. 2017.
[7] L. Fan, R. Kavasseri, Z. L. Miao, and C. Zhu, "Modeling of DFIG-based wind farms for SSR analysis," *IEEE Trans. Power Del.*, vol. 25, no. 4, pp. 2073–2082, Oct. 2010.
[8] Y. Cheng, L. Fan, J. Rose, S.-H. Huang, J. Schmall, X. Wang, X. Xie, J. Shair, J. R. Ramamurthy, N. Modi, C. Li, C. Wang, S. Shah, B. Pal, Z. Miao, A. Isaacs, J. Mahseredjian, and J. Zhou, "Real-world subsynchronous oscillation events in power grids with high penetrations of inverter-based resources," *IEEE Trans. Power Syst.*, vol. 38, no. 1, pp. 316–330, Jan. 2023.
[9] X. Xie, X. Zhang, H. Liu, H. Liu, Y. Li, and C. Zhang, "Characteristic analysis of subsynchronous resonance in practical wind farms connected to series-compensated transmissions," *IEEE Trans. Energy Convers.*, vol. 32, no. 3, pp. 1117–1126, Sep. 2017.
[10] L. Wang, X. Xie, Q. Jiang, H. Liu, Y. Li, and H. Liu, "Investigation of SSR in practical DFIG-based wind farms connected to a series-compensated power system," *IEEE Trans. Power Syst.*, vol. 30, no. 5, pp. 2772–2779, Sep. 2015.
[11] M. Abdeen, A. Emran, A. Moustafa, D. Kamal, R. Hassan, E. Hassan, F. Ahmed, M. Mahmoud, S. Kamel, and F. Jurado, "Investigation on TCSC parameters and control structure for SSR damping in DFIG-based wind farm," in *Proc. 12th Int. Renew. Energy Congr. (IREC)*, Oct. 2021, pp. 1–5.
[12] A. A. Emarloo, M. Changizian, and A. Shoulaie, "Application of gate-controlled series capacitor to mitigate subsynchronous resonance in a thermal generation plant connected to a series-compensated transmission network," *Int. Trans. Electr. Energy Syst.*, vol. 30, no. 12, p. e12673, 2020.
[13] L. Piyasinghe, Z. Miao, J. Khazaei, and L. Fan, "Impedance model-based SSR analysis for TCSC compensated type-3 wind energy delivery systems," *IEEE Trans. Sustain. Energy*, vol. 6, no. 1, pp. 179–187, Jan. 2015.
[14] L. F. W. De Souza, E. H. Watanabe, and J. E. D. R. Alves, "Thyristor and gate-controlled series capacitors: A comparison of components rating," *IEEE Trans. Power Del.*, vol. 23, no. 2, pp. 899–906, Apr. 2008.
[15] N. G. Hingorani and L. Gyugyi, *Understanding FACTS: Concepts and Technology of Flexible AC Transmission Systems*. New York, NY, USA: IEEE Press, 2000.
[16] A. Ahmadi, F. H. Gandoman, B. Khaki, A. M. Sharaf, and J. Pou, "Comprehensive review of gate-controlled series capacitor and applications in electrical systems," *IET Gener., Transmiss. Distrib.*, vol. 11, no. 5, pp. 1085–1093, Mar. 2017.
[17] L. A. S. Pilotto, A. Bianco, W. F. Long, and A. A. Edris, "Impact of TCSC control methodologies on subsynchronous oscillations," *IEEE Trans. Power Del.*, vol. 18, no. 1, pp. 243–252, Jan. 2003.
[18] F. D. D. Jesus, E. H. Watanabe, L. F. W. D. Souza, and J. E. R. Alves, "SSR and power oscillation damping using gate-controlled series capacitors (GCSC)," *IEEE Trans. Power Del.*, vol. 22, no. 3, pp. 1806–1812, Jul. 2007.
[19] M. R. A. Pahlavani and H. A. Mohammadpour, "Damping of subsynchronous resonance and low-frequency power oscillation in a series-compensated transmission line using gate-controlled series capacitor," *Electric Power Syst. Res.*, vol. 81, no. 2, pp. 308–317, Feb. 2011.
[20] H. A. Mohammadpour and E. Santi, "Modeling and control of gate-controlled series capacitor interfaced with a DFIG-based wind farm," *IEEE Trans. Ind. Electron.*, vol. 62, no. 2, pp. 1022–1033, Feb. 2015.
[21] H. A. Mohammadpour, A. Ghaderi, and E. Santi, "Analysis of subsynchronous resonance in doubly-fed induction generator-based wind farms interfaced with gate—Controlled series capacitor," *IET Gener., Transmiss. Distrib.*, vol. 8, no. 12, pp. 1998–2011, Dec. 2014.
[22] L. Fan and Z. Miao, "Mitigating SSR using DFIG-based wind generation," *IEEE Trans. Sustain. Energy*, vol. 3, no. 3, pp. 349–358, Jul. 2012.
[23] K. R. Padiyar, *FACTS Controllers in Power Transmission and Distribution*. New Delhi, India: New Age International, 2007.
[24] H. A. Mohammadpour, S. M. H. Mirhoseini, and A. Shoulaie, "Comparative study of proportional and TS fuzzy controlled GCSC for SSR mitigation," in *Proc. Int. Conf. Power Eng., Energy Electr. Drives*, Mar. 2009, pp. 564–569.
[25] Y. Bai and D. Wang, "Fundamentals of fuzzy logic control—Fuzzy sets, fuzzy rules and defuzzifications," in *Advanced Fuzzy Logic Technologies in Industrial Applications* (Advances in Industrial Control). Berlin, Germany: Springer, 2006, pp. 17–36.
[26] B. K. Bose, "Fuzzy logic and neural networks in power electronics and drives," *IEEE Ind. Appl. Mag.*, vol. 6, no. 3, pp. 57–63, May 2000.
[27] M. A. Hannan, Z. A. Ghani, A. Mohamed, and M. N. Uddin, "Real-time testing of a fuzzy-logic-controller-based grid-connected photovoltaic inverter system," *IEEE Trans. Ind. Appl.*, vol. 51, no. 6, pp. 4775–4784, Nov./Dec. 2015.
[28] M. Singh, P. Kumar, and I. Kar, "Implementation of vehicle to grid infrastructure using fuzzy logic controller," *IEEE Trans. Smart Grid*, vol. 3, no. 1, pp. 565–577, Mar. 2012.
[29] M. Abdeen, H. Li, and L. Jing, "Improved subsynchronous oscillation detection method in a DFIG-based wind farm interfaced with a series-compensated network," *Int. J. Electr. Power Energy Syst.*, vol. 119, Jul. 2020, Art. no. 105930.
[30] H. Li, M. Abdeen, Z. Chai, S. Kamel, X. Xie, Y. Hu, and K. Wang, "An improved fast detection method on subsynchronous resonance in a wind power system with a series compensated transmission line," *IEEE Access*, vol. 7, pp. 61512–61522, 2019.

MOHAMED ABDEEN received the B.Sc. and M.Sc. degrees in electrical engineering from Al-Azhar University, Cairo, Egypt, in 2011 and 2016, respectively, and the Ph.D. degree from Chongqing University, Chongqing, China, in 2020. He is currently an Assistant Professor with the Department of Electrical Engineering, Al-Azhar University. His research interests include power system stability, optimization, and control.

SAYED HOSNY AHMED EL-BANNA was born in Kafer El-Sheikh, Egypt, in July 1960. He received the B.Sc. (Hons.) and M.Sc. degrees in electrical engineering (power and machines sector) from Al-Azhar University, Egypt, in 1985 and August 1990, respectively, and the Ph.D. degree in electrical engineering (power and machines sector) from Al-Azhar University, in August 1997, according to the channel system between Berlin University and Al-Azhar University. His M.Sc. thesis was titled, "Load Flow Studies as an Affected by the Choice of the Slack Bus Bar" and the Ph.D. thesis was titled, "Design of an Expert System for the Evaluation of Power System Stability Through Pattern Recognition." Since 2003, he has been an Associate Professor with Al-Azhar University, where he has been a Professor, since 2008. He was a Professor with Umm Al-Qura University, Saudi Arabia, from 2008 to 2017. He has supervising and discussing more than 20 M.Sc. thesis and 11 Ph.D. thesis. He has excellent scientific cooperation with famous research institutes in Germany and Egypt through different funded research projects and thesis supervision. He has design and supervising on several projects with the General Organization for Physical Planning, Cairo, Egypt. He has published more than 32 technical papers in various international journals and conferences. His current research interests include control of power systems, power system transient stability, power system dynamic stability, power system security, multi-objective voltage control optimization, power system fault detection, load shedding, reactive power, voltage control, and power system restoration using artificial intelligence, such as expert systems, neural networks, and fuzzy controller and advanced engineering mathematics.

SARA ELGOHARY received the B.S. degree from the Department of Electrical Engineering, Faculty of Engineering, Al-Azhar University, in 2022. Her research interests include renewable energy systems and power system protection.

HEND MOSTAFA received the B.S. degree from the Department of Electrical Engineering, Faculty of Engineering, Al-Azhar University, in 2022. Her research interests include renewable energy systems and power system protection.

NORA GHALY received the B.S. degree from the Department of Electrical Engineering, Faculty of Engineering, Al-Azhar University, in 2022. Her research interests include renewable energy systems and power system protection.

NOURHAN ADEL received the B.S. degree from the Department of Electrical Engineering, Faculty of Engineering, Al-Azhar University, in 2022. Her research interests include renewable energy systems and power system protection.

ZEINAB ELKHWAS received the B.S. degree from the Department of Electrical Engineering, Faculty of Engineering, Al-Azhar University, in 2022. Her research interests include renewable energy systems and power system protection.

MOHAMED ALAHMADY received the B.S. degree from the Department of Electrical Engineering, Faculty of Engineering, Al-Azhar University, in 2022. His research interests include renewable energy systems and power system protection.

HOSSAM M. ZAWBAA received the B.Sc. and M.Sc. degrees from the Faculty of Computers and Information, Cairo University, Giza, Egypt, in 2008 and 2012, respectively, and the Ph.D. degree from Babeş-Bolyai University, Cluj-Napoca, Romania, in 2018. He is currently an Assistant Professor with the Faculty of Computers and Artificial Intelligence, Beni-Suef University, Beni Suef, Egypt. He has authored or coauthored more than 90 research publications in peer-reviewed reputed journals and international conference proceedings. His research interests include computational intelligence, machine learning, computer vision, and natural language understanding. He has been rated as one of the top 2% scientists worldwide by Stanford in the field of AI, for 2020, 2021, and 2022, respectively. Moreover, he has been awarded the State Encouragement Award in the field of engineering sciences from the Academy of Scientific Research and Technology, Egypt, in 2020.

SALAH KAMEL received the international Ph.D. degree from the University of Jaén, Spain (Main) and Aalborg University, Denmark (Host), in January 2014. He is currently an Associate Professor with the Department of Electrical Engineering, Aswan University. He is also a Leader of the Power Systems Research Group, Advanced Power Systems Research Laboratory (APSR Laboratory), Aswan, Egypt. His research interests include power system analysis and optimization, smart grid, and renewable energy systems.